Asociación Argentina
de Mecánica Computacional

Mecánica Computacional Vol XXXIX, págs. 367-376 (artículo completo)
F.E. Dotti, M. Febbo, S.P. Machado, M. Saravia, M.A. Storti (Eds.)
Bahía Blanca, 1-4 Noviembre 2022

ANALYSIS OF FLAME ONSET AND PROPAGATION FOR THE FLAME SPEED CLOSURE TURBULENT COMBUSTION MODEL IN CONSTANT-VOLUME VESSELS

Joaquín Aranciaga[a], Ezequiel J. López[a] and Norberto M. Nigro[b]

[a]*Instituto de Investigación en Tecnologías y Ciencias de la Ingeniería, Universidad Nacional del Comahue-CONICET, Buenos Aires 1400, 8300 Neuquén, Argentina*
joaquin.aranciaga@gmail.com, ezequiel.lopez@fain.uncoma.edu.ar

[b]*Centro de Investigación en Métodos Computacionales, Universidad Nacional del Litoral-CONICET, Predio CONICET "Dr. Alberto Cassano", Colectora RN 168 s/n – Paraje El Pozo, 3000 Santa Fe, Argentina*
norberto.nigro@cimec.santafe-conicet.gov.ar

Keywords: Computational Fluid Dynamics, Premixed Combustion, Turbulence, Ignition

Abstract. Computational simulations of the kernel growth resulting from a spark discharge in fuel-air mixtures have been carried out in many works to date by different groups, under both laminar and turbulent conditions. Within the Reynolds-Averaged Navier-Stokes (RANS) context, most turbulent combustion models in current and widespread use lack thorough testing and validation in a seemingly simple, though extremely valuable setup. Namely, a fan-stirred vessel with well-defined turbulence statistics, in which a spherical flame grows as it burns fresh mixture after a spark is discharged. A notable exception is the Flame Speed Closure (FSC) Model, which has been extensively employed to predict explosions under a wide range of conditions. The main focus of the present work is to examine a weak point associated to the model through the application of Computational Fluid Dynamics (CFD) for simulating turbulent combustion in constant-volume vessels, specifically the difficulty in producing successful ignitions using standard ignition models. A modification to circumvent the referred issue is proposed and assessed.

1 INTRODUCTION

Reynolds-Averaged Navier-Stokes (RANS) models have been, and still are, the standard approach in commercial codes for turbulent combustion simulations (Poinsot and Veynante, 2012). Arguably, the value of such models is directly related to their predictive capabilities, and therefore it is very important that they have the support provided by several tests on a variety of simple, well-defined cases covering their range of application. Experiments performed in fan-stirred bombs (or vessels) are normally very well-suited to test a model against. The rotating fans create a region of approximately statistically homogeneous, isotropic and stationary turbulence with zero mean flow. The turbulence intensity can be varied by adjusting the fan speed, and along with the fact that many apparatuses are prepared to withstand high initial pressures, a wide range of mixtures under different thermochemical and turbulent conditions can be explored. This is in contrast to main technological applications (e.g. internal combustion engines) where other phenomena, such as complex flow patterns or mixture inhomogeneity, hinder the analysis substantially. It is therefore reasonable that a first step in the development of any model consist in predicting the aforementioned simple problems. In this sense, the Flame Speed Closure (FSC) model proposed by Lipatnikov and Chomiak (1997) is conceivably the sole model shown to predict a large amount of well-defined experimental results with a slight (and well-justified) parameter tuning. In particular, it is among the few models that address the turbulent spreading of the mixture consistently with the classical Taylor's diffusion theory (Taylor, 1921). Nevertheless, the way the flame has been initialized may be deemed controversial. Although, as stated by the authors, the ignition submodel is not a part of the combustion model, it must possess some basic features which are not seen to be fulfilled, so far. For example, in the original derivation (Lipatnikov and Chomiak, 1997) an energy source is inserted into the enthalpy equation to simulate the energy supplied by the spark discharge. It is apparent that the specific power input term (expressed in W/m^3, consistent with the other terms in the differential equation) is multiplied by the density of the fresh mixture, breaking the basic dimensional consistency. This does not seem a misprint, since it is written in the same way in at least another paper (Lipatnikov and Chomiak, 2003). Moreover, in Lipatnikov and Chomiak (2004) the aforementioned specific power term is divided (rather than multiplied) by the same density, as is also the temporal derivative pressure term; both indeed seem misprints. A possible justification for the insertion of the fresh gas density as a factor in the power input source term is explored later in this work.

More confusion is added by noticing that in the original paper (Lipatnikov and Chomiak, 1997) the turbulent diffusivity in the enthalpy equation develops in time (as it should), but in subsequent works (Lipatnikov and Chomiak, 2003, 2004) it does not appear so. More recently (Huang et al., 2016) it does again, where additionally the way the mixture was ignited was changed without a proper explanation. In this paper methane-air explosions performed in a fan-stirred vessel by Haq (1998) are simulated to assess the performace of the FSC model. The aforementioned unclear issues are discussed and an alternative ignition model is proposed and tested to obtain improved agreement with the experimental data.

2 MODEL DESCRIPTION

2.1 Governing equations

This section introduces the conservation equations for the propagation of an unsteady, 1D (one-dimensional), statistically spherical turbulent flame in spherical coordinates. They closely follow the original presentation (Lipatnikov and Chomiak, 1997, 2003). Since pressure is as-

summed spatially uniform (though time-dependent) in the original formulation (and also retained here), the resolution of the momentum equation may be omitted. Hereafter, Reynolds (Favre) averages are represented by overbars (tildes) and subindex u (b) refers to a property evaluated on unburned (burned) gas.

- Continuity

$$\frac{\partial \bar{\rho}}{\partial t} + \frac{1}{r^2}\frac{\partial r^2 \bar{\rho}\tilde{u}}{\partial r} = 0 \tag{1}$$

where $\bar{\rho}$ is the density and $\tilde{u}$ is the velocity.

- Specific enthalpy ($\tilde{h}$)

$$\frac{\partial \bar{\rho}\tilde{h}}{\partial t} + \frac{1}{r^2}\frac{\partial r^2 \bar{\rho}\tilde{u}\tilde{h}}{\partial r} = \frac{1}{r^2}\frac{\partial}{\partial r}\left[r^2 \bar{\rho}(D_l + D_t)\frac{\partial \tilde{h}}{\partial r}\right] + \frac{\partial \bar{p}}{\partial t} + \dot{Q}_i \tag{2}$$

where $\bar{p}$ is the pressure, D_l is the heat diffusivity and D_t is the turbulent diffusivity, to be defined later. $\dot{Q}_i$ is an ignition source term, defined by

$$\dot{Q}_i = \frac{2E_{ign}}{\pi^{3/2}{\sigma_r}^3 t_{i,2}} \exp\left[-\left(\frac{r}{\sigma_r}\right)^2\right] \max\left[0, \min\left(\frac{t}{t_{i,1}}, \frac{t_{i,2}-t}{t_{i,2}-t_{i,1}}\right)\right] \tag{3}$$

The total ignition energy E_{ign} is inserted into the domain according to the spatial profile given by the exponential function, the extent of which is controlled by σ_r. The factor on the right (max/min) produces an ascending/descending ramp in time shaped by $t_{i,1}$ and $t_{i,2}$, the latter being the total discharge time. The reader should note that Eq. (3) is not multiplied by ρ_u, as done in the references, since this is considered inconsistent by physical and dimensional reasoning.

- Progress variable ($\tilde{c}$)

$$\frac{\partial \bar{\rho}\tilde{c}}{\partial t} + \frac{1}{r^2}\frac{\partial r^2 \bar{\rho}\tilde{u}\tilde{c}}{\partial r} = \frac{1}{r^2}\frac{\partial}{\partial r}\left[r^2 \bar{\rho}(D_l + D_t)\frac{\partial \tilde{c}}{\partial r}\right] + \underbrace{\rho_u V_t |\nabla \tilde{c}|}_{I} + \underbrace{\dot{Q}_l}_{II} + \underbrace{\dot{Q}_{i,c}}_{III} \tag{4}$$

The progress variable $\tilde{c}$ characterizes the mixture composition, being unity (zero) in completely burned (unburned) gas. The laminar diffusivity coincides with that of Eq. (2), which is valid for a unity Lewis number assumption. Terms I, II and III stand for turbulent, laminar-like and forced ignition sources, respectively. The developing turbulent burning velocity (V_t) and diffusivity (D_t) are given by

$$V_t = V_{t,\infty}\{1 + (\tau_L/t)[\exp(-t/\tau_L) - 1]\}^{1/2} \tag{5}$$

$$D_t = D_{t,\infty}[1 - \exp(-t/\tau_L)] \tag{6}$$

where $D_{t,\infty} = \nu_t/\sigma_t$, ν_t is the eddy diffusivity, σ_t is a turbulent Schmidt number (taken as unity here), $\tau_L = D_{t,\infty}/u'^2$ is the Lagrangian turbulent time scale, $V_{t,\infty} = Au'Da^{0.25}$ is the fully-developed turbulent burning velocity, $u' = \sqrt{\tilde{k}/1.5}$ is the rms turbulent velocity, $Da = (LS_l^2)/(u'D_{l,u})$ is the Damköhler number, S_l is the unstretched laminar burning

velocity and $L = C_D u'^3/\tilde{\epsilon}$ is an integral turbulent length scale. The correlation proposed by Amirante et al. (2017) is adopted for calculating S_l. The parameter $C_D = 0.37$ as in previous works (Lipatnikov and Chomiak, 1997, 2003). $\tilde{k}$ and $\tilde{\epsilon}$ are the specific turbulence kinetic energy and its dissipation, respectively.

The combustion model possesses a unique tunable constant A, and Q_l is given either by (Lipatnikov, 2012)

$$Q_l = \frac{\bar{\rho}(1-\tilde{c})}{t_r(1+D_t/D_{l,b})}\exp\left(-\Theta/\tilde{T}\right) \tag{7}$$

or

$$Q_l = \frac{\rho_u S_l^2}{4(D_{l,u}+D_t)}\tilde{c}(1-\tilde{c}) \tag{8}$$

where $\tilde{T}$ is the temperature, Θ = 20000 K is the activation temperature and t_r is a time scale adjusted so as to obtain the correct S_l for a laminar (i.e. $D_t = 0$), adiabatic, 1D, planar flame. It is important to note that Eq. (7) is capable of igniting the mixture, given that a source term in the enthalpy equation increases the temperature, while Eq. (8) is not. When using the latter, Eq. (7) was employed in Lipatnikov and Chomiak (2003, 2004) during a few milliseconds for igniting the mixture. Instead, in this case the following term is proposed in the present work:

$$Q_{i,c} = Str\rho_u(1-\tilde{c})\exp\left[-\left(\frac{r}{\sigma_c}\right)^2\right]\max\left[0,\min\left(\frac{t}{t_{i,1}},\frac{t_{i,2}-t}{t_{i,2}-t_{i,1}}\right)\right] \tag{9}$$

where the strength Str, the spatial parameter σ_c, $t_{i,1}$ and $t_{i,2}$ are specified in Section §3.

- Turbulence model (standard $k-\epsilon$, Launder and Spalding (1974))

$$\frac{\partial\bar{\rho}\tilde{k}}{\partial t} + \frac{1}{r^2}\frac{\partial r^2\bar{\rho}\tilde{u}\tilde{k}}{\partial r} = \frac{1}{r^2}\frac{\partial}{\partial r}\left[r^2\bar{\rho}(\nu_t/\sigma_k)\frac{\partial\tilde{k}}{\partial r}\right] + P_k - \bar{\rho}\tilde{\epsilon} \tag{10}$$

$$\frac{\partial\bar{\rho}\tilde{\epsilon}}{\partial t} + \frac{1}{r^2}\frac{\partial r^2\bar{\rho}\tilde{u}\tilde{\epsilon}}{\partial r} = \frac{1}{r^2}\frac{\partial}{\partial r}\left[r^2\bar{\rho}(\nu_t/\sigma_\epsilon)\frac{\partial\tilde{\epsilon}}{\partial r}\right] + C_{\epsilon,1}\frac{\tilde{\epsilon}}{\tilde{k}}P_k - C_{\epsilon,2}\bar{\rho}\frac{\tilde{\epsilon}^2}{\tilde{k}} \tag{11}$$

$$P_k = (2/3)\bar{\rho}[2\nu_t(\partial\tilde{u}/\partial r - \tilde{u}/r)^2 - (\tilde{k}/r^2)\partial(r^2\tilde{u})/\partial r] \tag{12}$$

The eddy diffusivity is computed as $\nu_t = C_\mu\tilde{k}/\tilde{\epsilon}$ and the model parameters are $C_\mu = 0.09$, $C_{\epsilon,1} = 1.44$, $C_{\epsilon,2} = 1.92$, $\sigma_k = 1$, and $\sigma_\epsilon = 1.3$.

The system of equations is closed using the equation of state

$$\bar{\rho} = \bar{p}/[R_u T_u(1-\tilde{c}) + R_b T_b\tilde{c}] \tag{13}$$

where R_u and R_b are the gas constants for fresh and burned mixtures, respectively.

2.2 Thermophysical and transport properties

The laminar diffusivity is computed as $D_l = D_{l,0}(T/T_0)^{1.7}(p_0/p)$, with $D_{l,0} = 0.225$ cm^2/s, $T_0 = 300$ K and $p_0 = 1$ bar. The molar mass (M), specific heat at constant pressure (c_p) and enthalpy of formation (h_f) are constants for fresh and burned mixtures, but different between them. They were computed by fitting with a first-degree polynomial the enthalpy and internal energy of a stoichiometric methane-air mixture computed using an equilibrium code (Ferguson and Kirkpatrick, 2016) over 1-10 bar and 300-1500 K (1700-2300 K) for fresh (burned) mixtures. The resulting properties are $c_{p,u} = 1.28$ kJ/(kg·K), $h_{f,u} = -0.675$ MJ/kg, $M_u = 27.6$ kg/kmol, $c_{p,b} = 1.73$ kJ/(kg·K), $h_{f,b} = -4.15$ MJ/kg, $M_b = 26.9$ kg/kmol.

2.3 Initial and boundary conditions

Two different setups are distinguished at this point. In Section §3 a 1D planar flame propagating in frozen turbulence is firstly run in cartesian coordinates. The advantage of such a configuration is that an analytical solution exists when D_l and Q_l are both null, thereby being used as a reference for code validation. Initialization for this case is carried out by imposing the analytical solution of the progress variable (Eq. (15)) a short time after discharge:

$$\tilde{c}(x, t_0) = \frac{\rho_b \bar{c}}{\bar{\rho}} = \frac{\rho_b}{\bar{\rho}} 0.5 \operatorname{erfc}\left(\frac{x - x_0}{\delta_{t,0}/\sqrt{\pi}}\right) \tag{14}$$

where x_0 is the initial position of the flame [1] (at $\bar{c} = 0.5$) and $\delta_{t,0}$ is the turbulent flame brush thickness, computed via Eq. (16). To attain a sufficient spatial resolution with a reasonable number of cells, $t_0 = 100$ μs is chosen here. Zero-gradient boundary conditions are applied at both boundaries for every field, except for the velocity at $x = 0$, which is null.

For the simulations in spherical coordinates of the experiments performed by Haq (1998), the initial conditions are $\tilde{c} = 0$, $\tilde{u}(r, t_0) = 0$, $\tilde{k}(r, t_0) = 1.5u_0'^2$ and $\tilde{\epsilon}(r, t_0) = 0.37u_0'^3/L$. All spatial gradients are zero at r = R$_{max}$, where R$_{max}$ is the bomb radius. Since the reported experimental results correspond to the pre-pressure period, pressure can be considered constant not only in space, but also in time ($\partial p/\partial t = 0$ in Eq. (2)), with very little error. This allows to run in a reduced domain, large enough so that every field tends to zero before reaching the boundary. The domain is increased in size as the flame grows. This strategy also renders redundant the solution of Eq. (2) whenever $Q_i = 0$, since $\tilde{h}$ is constant in space and time, further lowering the computational cost.

2.4 Solution strategy

The partial differential equations are integrated and discretized employing the Finite Volume Method, coded in an in-house program. Central difference and Crank-Nicolson schemes are used in space and time, respectively, being both second-order accurate. Face values are obtained via linear interpolation. The time step $\Delta t = 0.5$ μs and cell size $\Delta r = 20$ μm are adopted throughout this work, both verified to yield temporal and spatial independence.

3 RESULTS AND DISCUSSION

Results of the code implementation are validated in this section, followed by testing of the FSC model against the experimental data presented by Haq (1998).

[1] For the statistically planar flame the radial coordinate r is replaced by a cartesian coordinate x, and the governing equations introduced in Section §2.1 are re-expressed in cartesian coordinates.

3.1 Validation case

A 1D planar flame in frozen turbulence ($u' = 2.38$ m/s and $L = 20$ mm) is employed as a reference case to validate the code, for it possesses an exact analytical solution when D_l and Q_l are null in Eq. (4) (Lipatnikov, 2012):

$$\bar{c} = 0.5\,\mathrm{erfc}\left(\frac{x - x_f}{\delta_t/\sqrt{\pi}}\right) \tag{15}$$

$$\delta_t^2 = 4\pi D_{t,\infty} t \left\{1 - \frac{\tau_L}{t}\left[1 - \exp\left(-\frac{t}{\tau_L}\right)\right]\right\} \tag{16}$$

$$x_f(t) = x_f(t = t_0) + \int_0^t V_t dt' \tag{17}$$

The flame brush thickness is calculated from the simulation results as $\delta_t = [\max(|\nabla \bar{c}|)]^{-1}$ and the global burning velocity $U_t = (\rho_b/\rho_u) dx_f/dt$, where x_f corresponds to the spatial location of $\bar{c} = 0.5$. The former is normalized by $\sqrt{2\pi}L$ and the latter by $V_{t,\infty}$, and both are plotted in Fig. 1, where an almost perfect agreement with Eqs. (16) and (5) is obtained. The figure also reveals a key distinctive feature of the FSC model: the different developments of the flame brush thickness and burning velocity.

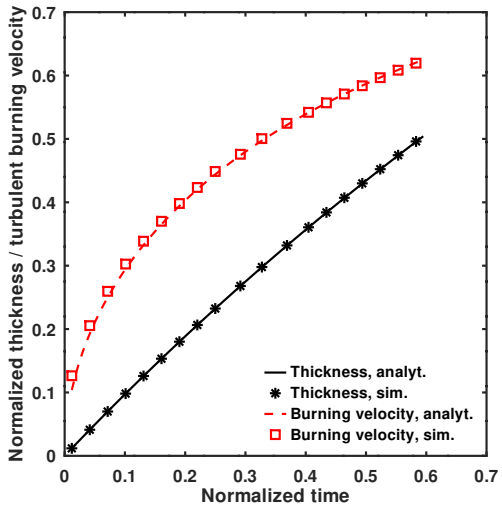

Figure 1: Analytical (lines) and simulated (symbols) normalized turbulent flame brush thickness and burning velocity vs. time.

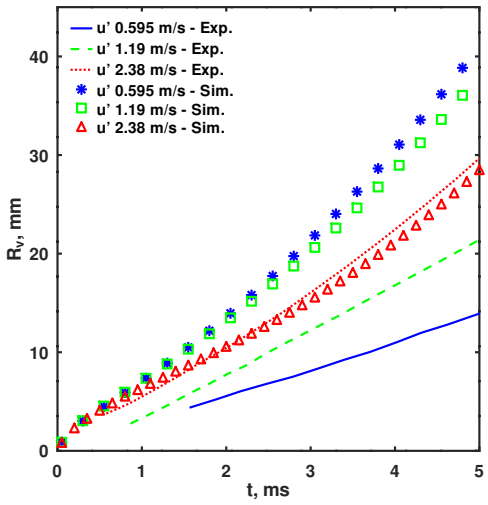

Figure 2: Experimental (lines) vs. simulated (symbols) burned radii vs. time at $p = 1$ bar and $u' = 0.595$, 1.19 and 2.38 m/s using the submodel provided by Eqs. (7) and (3).

3.2 Experimental cases

Experimental data presented by Haq (1998) were selected to test the model against, because it covers three rms turbulent velocities (u' = 0.595, 1.19 and 2.38 m/s) and two different initial pressures (1 and 5 bar). Moreover, as the mixture is stoichiometric methane/air, non-unity Lewis number and preferential diffusion effects are minimized and can be neglected. The discharged ignition energy was estimated to be approximately 23 mJ, although only a fraction of it would

have been effectively transfered to the gas. The discharge duration was not reported, and the spark gap was 1 mm for $p = 1$ bar and 0.6 mm for $p = 5$ bar.

The first set of simulations is performed with the laminar-like source term submodel given by Eq. (7). The ignition energy E_{ign} is taken identical to the reported experimental value, keeping in mind that it represents only an approximation. The discharge parameters $t_{i,1} = 0.1$ ms and $t_{i,2} = 1$ ms are chosen to be close to previous works (Lipatnikov and Chomiak, 1997, 2003). The only tunable parameter of the model is $A = 0.4$, identical to that adopted in the aforesaid works when using Eq. (7). Only ignitions at $p = 1$ bar are simulated with this submodel, since at $p = 5$ bar the kernel for the highest turbulent case is quenched short after discharge, even multiplying Eq. (3) by ρ_u, as done in the aforementioned references. Figure 2 shows, for the three different values of u', the temporal evolution of burned radii R_v, defined in such a way that spheres delimited by R_v contain equal volumes of unburned gas within, than volumes of burned gas outside of it.[2] It can be noticed that the high turbulence case is the only one well resolved, whereas the lower turbulence cases exhibit higher flame speeds, contrary to the experimental data. These results qualitatively agree with those presented in Lipatnikov and Chomiak (2003) (c.f. Fig. 5 in the referenced paper). Beyond the quantitative differences, seeing that the trend is wrongly reproduced calls into question the merit of Eq. (7). Such term has not impeded a correct trend with u' in Huang et al. (2020), but among other adjustments, the fact that turbulence was kept frozen for the first couple of milliseconds prevents a direct analogy with out results. The submodel given by Eq. (7) was adopted from laminar flame theory, and it permits the turbulent combustion model (Eq. (4)) to tend to a laminar flame equation as $u' \to 0$. The issue encountered here with the submodel is probably due to the combination of turbulence and mean flame curvature (κ_m). Without the former, u' = 0 and Eq. (4) represents a plausible basic laminar flame, given that it can be well-represented by simplified chemistry and ignoring differential and preferential diffusion effects. Without the latter (i.e. the flame is statistically plane) the submodel impedes an infinite growth of the flame brush thickness (which is physically correct) and increases the propagation speed by an amount equal to S_l. As there is no curvature, the flame speed is not dependent on flame geometry. When both u' and κ_m are not zero, the interplay between the increased flame thickness due to turbulent diffusion and mean curvature greatly reduces the flame speed, which forces an augmentation of the necessary ignition energy to avoid flame quenching. This effect is worsen by a higher u', but also by a higher pressure, since in this case the ratio δ_t/δ_l is increased at a constant u', where δ_l is the laminar flame thickness. This may be the reason why the FSC developers multiplied Eq. (3) by ρ_u. Regarding the turbulent diffusivity in the enthalpy equation (Eq. (2)), a few tests performed under different conditions revealed that without the development described by Eq. (6) the temperature increase following the spark discharge is rapidly dissipated, rendering almost impossible a successful ignition, supporting the original expression of the enthalpy equation (Lipatnikov and Chomiak, 1997).

Considering that the submodel given by Eq. (7) does not seem to behave properly, it is replaced by Eq. (8). Rather than igniting the mixture with Eqs. (3) and (7), the ignition model given by Eq. (9) is tested next. In addition, a spatial modification to the turbulent diffusivity is applied, rendering Eq. (6) into

$$D_t = D_{t,\infty}[1 - \exp(-t/\tau_L)][1 - \exp(-r/\sigma_i)] \tag{18}$$

where the spatial parameter σ_i = 5 mm reduces the effective turbulent diffusivity in the vicinity of the spark gap. The parameters Str, σ_c, $t_{i,1}$ and $t_{i,2}$ are selected as small as possible to reduce

[2]The reader is referred to Bradley et al. (2003), for example, for a better understanding of this definition.

the influence of the ignition submodel on the subsequent flame propagation. Their values are σ_c = 0.25 mm, $t_{i,1}$ = 0.1ms, $t_{i,2}$ = 0.5 ms and the strength, as explained in the following, is made dependent on the initial u': $Str = 10^5(u_0'^2 + 0.1)$, where u_0' is expressed in m/s and the resulting Str has units s^{-1}. The model's tunable parameter is A = 0.45, slightly less than A = 0.5 used in conjunction with Eq. (8) in other works. Figures 3 and 4 show the temporal evolution of burned radii at 1 and 5 bar, respectively, for the different u'. The experimental behavior at low pressure is very well reproduced by the simulations, while that at high pressure could be deemed acceptable, particularly for the two highest u'. An important feature of the FSC model can also be noticed in these figures, which is its capability to show opposite effects of pressure on turbulent and laminar burning velocities, as observed in experiments (Kobayashi et al., 1996, 1998). In the case of methane, pressure does not have a marked influence on turbulent burning velocity because the reduction of S_l with pressure is substantial, and almost compensates the velocity increase brought about by the reduction of $D_{l,u}$ with pressure. The turbulence dependence of the ignition term (Eq. (9)) emerges as a need to increase the turbulence generation for the higher u' cases, in relation to the lower u' case. Otherwise, the turbulence evolution for the low u' case makes it grow too fast, a result probably inherited by the inadequacy of the $k - \epsilon$ turbulence model when used with this type of problems, for which it was neither designed nor correctly validated, despite its extended usage. Figures 5 and 6 depict the flame structure for the cases $u' = 0.595$ m/s - 1 bar and $u' = 2.38$ m/s - 5 bar, respectively, at three different instants of time. The computed flame shapes are self-similar, as the model is intended to yield. The fact that some experimental profiles do not evidence this shape is thought to respond to the consideration that more experimental realizations need to be executed for the sample average to tend to the true average. All in all, the general agreement in the flame structure is rather adequate. An important statement regarding the ignition submodel given by Eq. (9) is that by no means it is intended that such a simple representation be suitable for all posible experimental rigs and thermophysical and turbulence conditions. It's been proven here to work quite well with the present experimental data, but more thorough examination is required for general application purposes.

4 CONCLUSIONS

The Flame Speed Closure (FSC) model for simulating turbulent combustion has been implemented in an in-house code, followed by its validation and testing against experimental data gathered from explosions in a fan-stirred vessel, spanning variations in turbulence velocity and pressure, which constitutes a well-defined configuration. Its most relevant features have been discussed and issues associated with the mixture ignition under conditions of moderate/high turbulence and pressures have been reported, and the causes for them, elucidated. The most prominent points to be outlined are the following:

- The laminar-like term given by Eq. (7) along with the ignition submodel given by Eq. (3) does not perform well for the conditions of the present work.
- The laminar-like term given by Eq. (8), along with the simple ignition submodel given by Eq. (9) is supported for the present conditions, although more extensive testing is required to determine the coefficients of Eq. (9).
- The turbulent diffusivity in the enthalpy equation must develop in time to yield reasonable results, although this is particularly important when igniting the mixture with an energy source term.

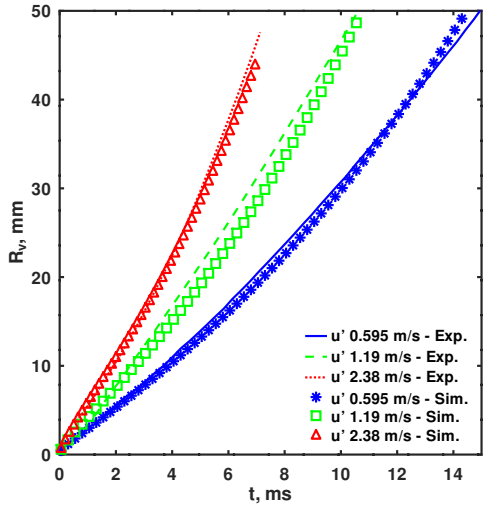

Figure 3: Experimental (lines) vs. simulated (symbols) burned radii vs. time at $p = 1$ bar and $u' = 0.595$, 1.19 and 2.38 m/s using the submodel provided by Eqs. (8) and (9).

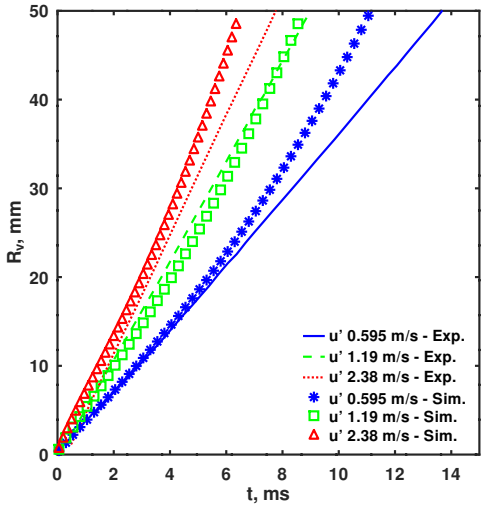

Figure 4: Experimental (lines) vs. simulated (symbols) burned radii vs. time at $p = 5$ bar and $u' = 0.595$, 1.19 and 2.38 m/s using the submodel provided by Eqs. (8) and (9).

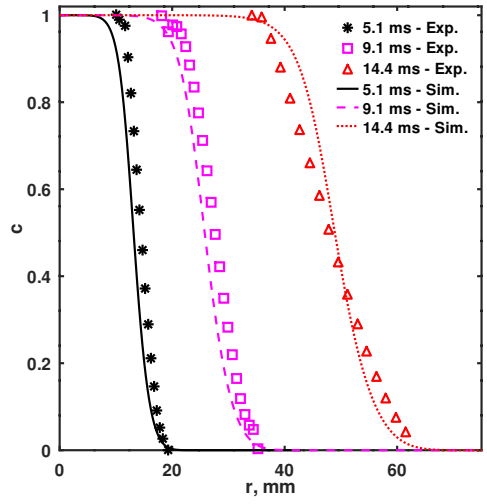

Figure 5: Experimental (symbols) and simulated (lines) turbulent flame structure, given by spatial profiles of $\bar{c}$, for $p = 1$ bar and $u' = 0.595$ m/s.

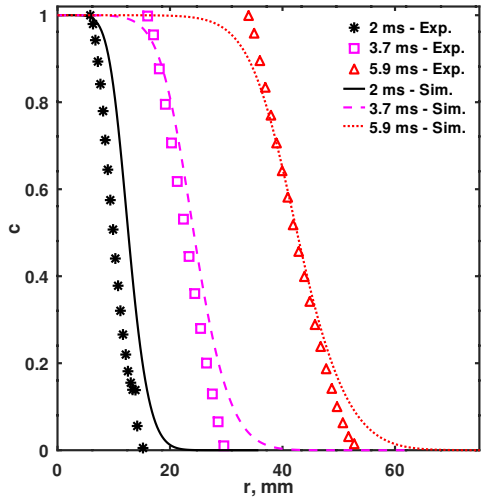

Figure 6: Experimental (symbols) and simulated (lines) turbulent flame structure, given by spatial profiles of $\bar{c}$, for $p = 5$ bar and $u' = 2.38$ m/s.

REFERENCES

Amirante R., Distaso E., Tamburrano P., and Reitz R.D. Laminar flame speed correlations for methane, ethane, propane and their mixtures, and natural gas and gasoline for spark-ignition engine simulations. *International Journal of Engine Research*, 18(9):951–970, 2017.

Bradley D., Haq M.Z., Hicks R.A., Kitagawa T., Lawes M., Sheppard C.G.W., and Woolley R. Turbulent burning velocity, burned gas distribution, and associated flame surface definition. *Combust. Flame*, 133:415–430, 2003.

Ferguson C. and Kirkpatrick A. *Internal Combustion Engines: Applied Thermosciences*. 3 edition, 2016.

Haq M.Z. *Fundamental studies of premixed combustion*. Ph.D. thesis, The University of Leeds, 1998.

Huang C., Lipatnikov A.N., and Nessvi K. Unsteady 3-d rans simulations of dust explosion in a fan stirred explosion vessel using an open source code. *Journal of Loss Prevention in the Process Industries*, 67:104237, 2020.

Huang C., Yasari E., Johansen L.C.R., Hemdal S., and Lipatnikov A.N. Application of flame speed closure model to rans simulations of stratified turbulent combustion in a gasoline direct-injection spark-ignition engine. *Combustion Science and Technology*, 188(1):98–131, 2016.

Kobayashi H., Kawabata Y., and Maruta K. Experimental study on general correlation of turbulent burning velocity at high pressure. *Symposium (International) on Combustion*, 27(1):941–948, 1998. Twenty-Seventh Sysposium (International) on Combustion Volume One.

Kobayashi H., Tamura T., Maruta K., Niioka T., and Williams F.A. Burning velocity of turbulent premixed flames in a high-pressure environment. *Symposium (International) on Combustion*, 26(1):389–396, 1996.

Launder B.E. and Spalding D.B. The numerical computation of turbulent flows. *Computer Methods in Applied Mechanics and Engineering*, 3(2):269–289, 1974.

Lipatnikov A.N. *Fundamentals of Premixed Turbulent Combustion*. CRC Press, 2012.

Lipatnikov A.N. and Chomiak J. A simple model of unsteady turbulent flame propagation. *SAE Technical Paper*, 972993, 1997.

Lipatnikov A.N. and Chomiak J. A numerical study of weakly turbulent premixed combustion with flame speed closure model. *SAE Technical Paper*, 2013-01-1839, 2003.

Lipatnikov A.N. and Chomiak J. Flame speed closure model of premixed turbulent combustion : Further development and validation(s.i. engines, flame propagation). *The international symposium on diagnostics and modeling of combustion in internal combustion engines*, 2004.6:583–590, 2004.

Poinsot T. and Veynante D. *Theoretical and Numerical Combustion*. Poinsot T. and Veynante D., 3 edition, 2012.

Taylor G. Diffusion by continuous movements. *Proc. Lond. Math*, (20):196–212, 1921.